



*Using CO₂ Lidar for Standoff Detection of a
Perfluorocarbon Tracer in Air*

John Heiser, Scott Smith and Arthur Sedlacek III

September 2008

**Environmental Sciences Department/Environmental Research &
Technology Division**

Brookhaven National Laboratory

P.O. Box 5000
Upton, NY 11973-5000

www.bnl.gov

Notice: This manuscript has been authored by employees of Brookhaven Science Associates, LLC under Contract No. DE-AC02-98CH10886 with the U.S. Department of Energy. The publisher by accepting the manuscript for publication acknowledges that the United States Government retains a non-exclusive, paid-up, irrevocable, world-wide license to publish or reproduce the published form of this manuscript, or allow others to do so, for United States Government purposes.

DISCLAIMER

This report was prepared as an account of work sponsored by an agency of the United States Government. Neither the United States Government nor any agency thereof, nor any of their employees, nor any of their contractors, subcontractors, or their employees, makes any warranty, express or implied, or assumes any legal liability or responsibility for the accuracy, completeness, or any third party's use or the results of such use of any information, apparatus, product, or process disclosed, or represents that its use would not infringe privately owned rights. Reference herein to any specific commercial product, process, or service by trade name, trademark, manufacturer, or otherwise, does not necessarily constitute or imply its endorsement, recommendation, or favoring by the United States Government or any agency thereof or its contractors or subcontractors. The views and opinions of authors expressed herein do not necessarily state or reflect those of the United States Government or any agency thereof.

Using CO₂ Lidar for Standoff Detection of a Perfluorocarbon Tracer in Air
John Heiser, Scott Smith and Arthur Sedlacek III

Abstract.....	2
1.0 Summary.....	2
2.0 Introduction.....	3
3.0 Lidar Background, System Design, Assembly and Optimization	3
3.1 Lidar Design	5
3.2 Laboratory Testing.....	7
3.3 Indoor Testing.....	9
3.4 Outdoor Optimization	9
4.0 Demonstration Results and Discussion.....	14
4.1 Results.....	14
5.0 Conclusions.....	16
6.0 Recommendations.....	16
7.0 References.....	18
Figure 1 Schematic of Typical Lidar System	4
Figure 2 Differential Absorption Lidar.....	5
Figure 3 Lidar Platform used for PFT Detection (output side).....	6
Figure 4 Lidar Platform used for PFT Detection (collection side).....	6
Figure 5 Schematic of Lidar Platform used for Testing and Demonstration of PFT Detection in Air.....	7
Figure 6 Laboratory Apparatus used in Calibrating PFT Lidar.....	8
Figure 7 Lidar Test Facility showing Beam Path	10
Figure 8 CONOPS for Standoff Detection of PFTs	11
Figure 9 Graphical Interface for PFT Lidar.....	12
Figure 10 Results of Outdoor Testing of Lidar.....	13
Figure 11 Lidar Field Demonstration Set up	14
Figure 12 Lidar Output for the August 27th Demonstration of Stand-off detection of PFTs	15
Figure 13 Dual Wavelength (dual laser) Lidar for PFT Stand-off Detection	17
Figure 14 Off Axis Optical Lidar Configuration versus Standard Lidar Configuration...	17

Abstract

The Tag, Track and Location System Program (TTL) is investigating the use of PFTs as tracers for tagging and tracking items of interest or fallen soldiers. In order for the tagging and tracking to be valuable there must be a location system that can detect the PFTs. This report details the development of an infrared lidar platform for standoff detection of PFTs released into the air from a tagged object or person. Furthering work performed using a table top lidar system in an indoor environment; a mobile mini lidar platform was assembled using an existing Raman lidar platform, a grating tunable CO₂ IR laser, Judson HgCdTe detector and miscellaneous folding optics and electronics. The lidar achieved ~200 ppb-m sensitivity in laboratory and indoor testing and was then successfully demonstrated at an outdoor test. The lidar system was able to detect PFTs released into a vehicle from a distance of 100 meters. In its final, fully optimized configuration the lidar was capable of repeatedly detecting PFTs in the air released from tagged vehicles. Responses were immediate and clear.

1.0 Summary

This report details the results of a proof-of-concept demonstration for standoff detection of a perfluorocarbon tracer (PFT) using infrared lidar. The project is part of the Tag, Track and Location System Program and was performed under a contract with Tracer Detection Technology Corp. with funding from the Office of Naval Research. A lidar capable of detecting PFT releases at distance was assembled by modifying an existing Raman lidar platform by incorporating a grating tunable CO₂ IR laser, Judson HgCdTe detector and miscellaneous folding optics and electronics. The lidar achieved ~200 ppb-m sensitivity in laboratory and indoor testing and was successfully demonstrated at an outdoor test. The demonstration test (scripted by the sponsor) consisted of three parked cars, two of which were tagged with the PFT. The cars were located 70 (closest) to 100 meters (farthest) from the lidar (the lidar beam path was limited by site constraints and was ~100 meters). When one door of each of the cars was opened (sequentially), the lidar was clearly able to determine which vehicles had been tagged and which one was not. The lidar is probably capable of greater than 0.5 kilometer standoff distances based on the extreme amount of signal return achieved (so much that the system had to be de-tuned).

The BNL lidar system, while optimized to the extent possible with available parts and budget, was not as sensitive as it could be. Steps to improve the lidar are detailed in this report and include using a better laser system (for more stable power output), dual wavelengths (to improve the sensitivity and allow common mode noise reduction and to allow the use of the lidar in a scanning configuration), heterodyning (for range resolved PFT detection) and an off-axis optical configuration (for improved near field sensitivity).

2.0 Introduction

Perfluorocarbon tracers (PFTs) are colorless, odorless compounds that consist of carbon and fluorine atoms joined by covalent single bonds. These compounds are chemically inert, non-flammable, and have no biological effects. There are several PFTs that make

suitable tracers. Background levels of these PFTs are in the parts per quadrillion (10^{15}) and have remained relatively constant at this low level over the past 4 decades. PFTs have been used as atmospheric tracers, for leak location, building infiltration measurements, subsurface environmental investigations and many other applications over the last few decades.

Historically, PFTs have been analyzed via gas chromatography (GC) using an electron capture detector. GC methods are capable of part per quadrillion detection limits and can measure multiple PFTs simultaneously in 15 minutes or less. In 2001 to 2002, as an alternative to conventional GC analysis, a laser-based, infrared CO₂ lidar system was developed by Brookhaven National Laboratory (BNL). BNL developed a table mounted lidar system that achieved 1 ppb-m resolution in an indoor controlled environment¹. The advantages of lidar versus conventional GC methods include standoff detection, a path integrated analysis and real-time results. The major disadvantages include much reduced sensitivity and atmospheric interferences.

The Tag, Track and Location System Program (TTL) is investigating the use of PFTs as tracers for tagging and tracking items of interest or fallen soldiers. In order for the tagging and tracking to be valuable there must be a location system that can detect the PFTs. Two types of detection are needed; the first is proximity detectors and the second standoff detectors that can detect the PFTs from a distance or remote/hidden point. This project (as part of the TTL), looks to further the development of CO₂ lidar for standoff detection of airborne PFTs by extending laboratory-based measurements conducted earlier to the field. The laboratory-based lidar developed in 2002 by Heiser and Sedlacek¹ was translated to an existing mini-lidar platform originally used for a Raman lidar² to allow rapid development of a fieldable CO₂ lidar suitable for the detection of outdoor releases of PFT. This report details the design of the lidar system, pretesting and optimization of the system prior to the demonstration and reports the results of a field demonstration of the lidar held August 27, 2008 at BNL.

3.0 Lidar Background, System Design, Assembly and Optimization

At its most fundamental level, lidar is simply the optical analog of radar. Just as in radar, there is a transmitter, a receiver and data processing subunit. Figure 1 shows a schematic of the BNL mini-Raman Lidar System³ (MRLS) platform which, while specific to Raman lidar, contains the basic elements of lidar. The optical receiver telescope is typically either of a Cassegrainian or Newtonian design though other designs have been used. The collected return signal can then be sent to a variety of detection subsystems depending upon the desired information.

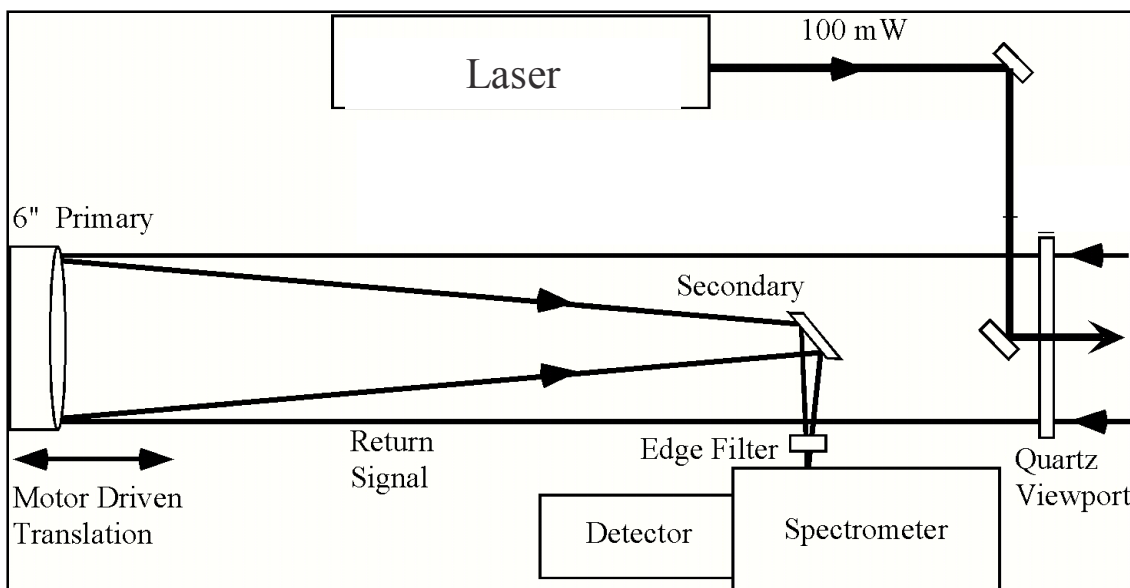


Figure 1 Schematic of Typical Lidar System

The phenomena that lidar platforms can exploit fall into two general categories, elastic scattering (for absorption measurements and aerosol density profiles) and inelastic scattering (fluorescence and Raman spectroscopy). For chemical species detection and monitoring, the phenomenon of choice in the atmospheric community is primarily absorption by specific target molecules due to the availability of large absorption cross-sections in readily accessible laser wavelengths. Leveraging these advantages translates to high-detection sensitivities on the order of low parts-per-million (ppm)^{4,5,6} to low parts-per-billion (ppb) levels^{7,8}. This type of absorption measurement is accomplished by using the differential absorption approach commonly referred to as DIAL (Differential Absorption Lidar)^{9,10,11}. As the name suggests, the implementation of DIAL involves using two laser frequencies that are directed to the area of interest and their respective elastic return signals monitored: λ_1 located at a highly-absorbing wavelength for the chemical species-of-interest and λ_2 in a non-absorbing spectral region, as shown in Figure 2. Elastic return of each outgoing laser line (λ_1 and λ_2) is provided through either a combination of Rayleigh scattering off air molecules and Mie scattering from the aerosols/particulates or, if range-resolved mapping is not important, hard-body return from a retroreflector [e.g., corner cube or a sand-blasted aluminum back-drop]. The lidar platform used in this present study is DIAL.

The original tabletop-lidar system was developed under a BNL Laboratory Directed Research and Development program. This system was a proof-of-concept demonstration of stand-off detection of PFTs using an IR laser. The proposed end use of the lidar was the detection of leaks in cap/cover systems for waste landfills. The project and results are detailed elsewhere (see Heiser and Sedlacek, 2005), but in summary, 1 ppb-m resolution over 40 meters in a controlled indoor environment was achieved. The focus of this project was to further this previous work by mounting the lidar on a mini-platform that would allow the system to be portable/mobile. BNL had also previously developed a mini Raman lidar³ and the platform from that system was utilized as a time and cost saving measure. The objective of BNL's portion of this project was to demonstrate proof-of-

concept for developing a portable IR lidar and to attempt to bound the resolution limits of IR lidar standoff detection of a PFT; perfluoromethylcyclohexane (PMCH).

3.1 Lidar Design

As alluded to above, the CO₂ lidar system used in the present research effort utilized an existing Raman lidar platform. This saved several months of designing/machining and ~\$150K in material costs. Figure 1 depicts a typical lidar set up consisting of the laser, folding optics, a primary collection mirror and detector, as introduced earlier.

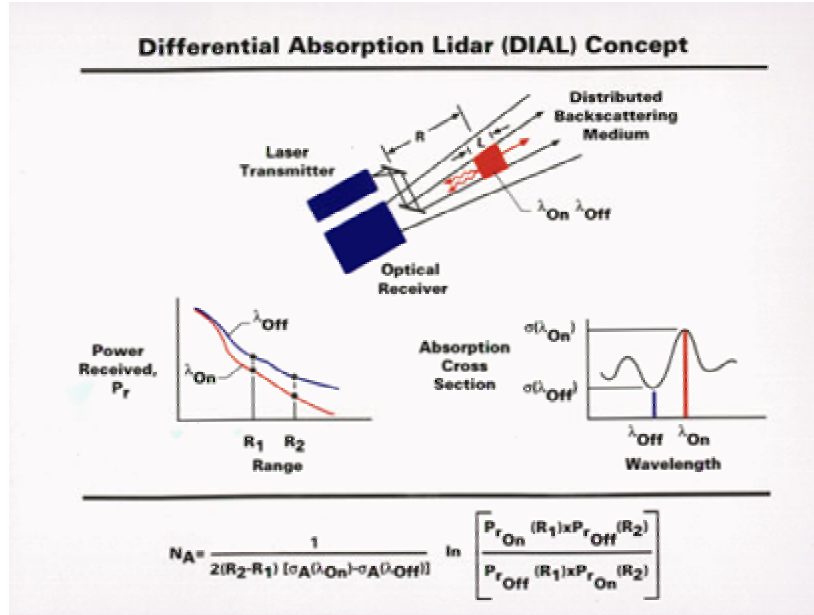


Figure 2 Differential Absorption Lidar

The internal platform consists of a lightweight, honeycomb construction aluminum panel that the laser, optics and detector are mounted on. The panel is set on a sturdy tripod (see Figures 2 & 3). For simplicity, the electronics (24 bit A/D card, power transformer for the lidar and electronic beam chopper) were mounted externally and cables were used to connect to the platform. The UV optics were removed and replaced with IR specific folding optics. This included machining and mounting custom optic holders.

The IR lidar platform is also of interest to BNL for environmental investigation. As such, BNL, through program development, purchased a CO₂ laser to help further develop IR lidar. This program was able to leverage this and used the laser in this project. The laser, from Access Laser Company, is a grating tunable (adjustable wavelength) CO₂ IR Model MERIT-G. It was delivered with cold plate cooling to allow stand alone operation without external cooling. [This option later proved inadequate for the demands of lidar and a water cooling option was incorporated.] The advertised specifications are:

Wavelength range: 9.2 μm to 10.8 μm (at least 50 lines)

Power: 28 VDC, 7 amps

Laser Power: 2 watts continuous at peak lines

Power stability: 5% Typical for the strong lines

Laser mode: Near TEM₀₀, M² < 1.1; beam dia. 2.4 mm, full divergence angle 5.5 mrad

Lase Head Dimensions: 16" x 4.1" x 2.8"



Figure 3 Lidar Platform used for PFT Detection (output side)



Figure 4 Lidar Platform used for PFT Detection (collection side)

The MERIT G system included the laser, a controller (safety module with safety key switch, safety interlock and power adjustment) and the RF power supply. Later on, a power meter was added to allow normalization of the input signal to the laser output. The power meter attached directly to the front of the laser and sends 3% of the laser output to the power meter and the remainder as output beam. Gold mirrors were used to fold the outgoing IR laser beam into the receiver field-of-view. A ZnSE window was also incorporated into the optical path so that the output from a HeNe laser could be used for both near and far-field alignment. A Judson series J15D HgCdTe detector was used in the lidar. A schematic of the unit as it was used in the testing and demonstration is depicted in Figure 5.

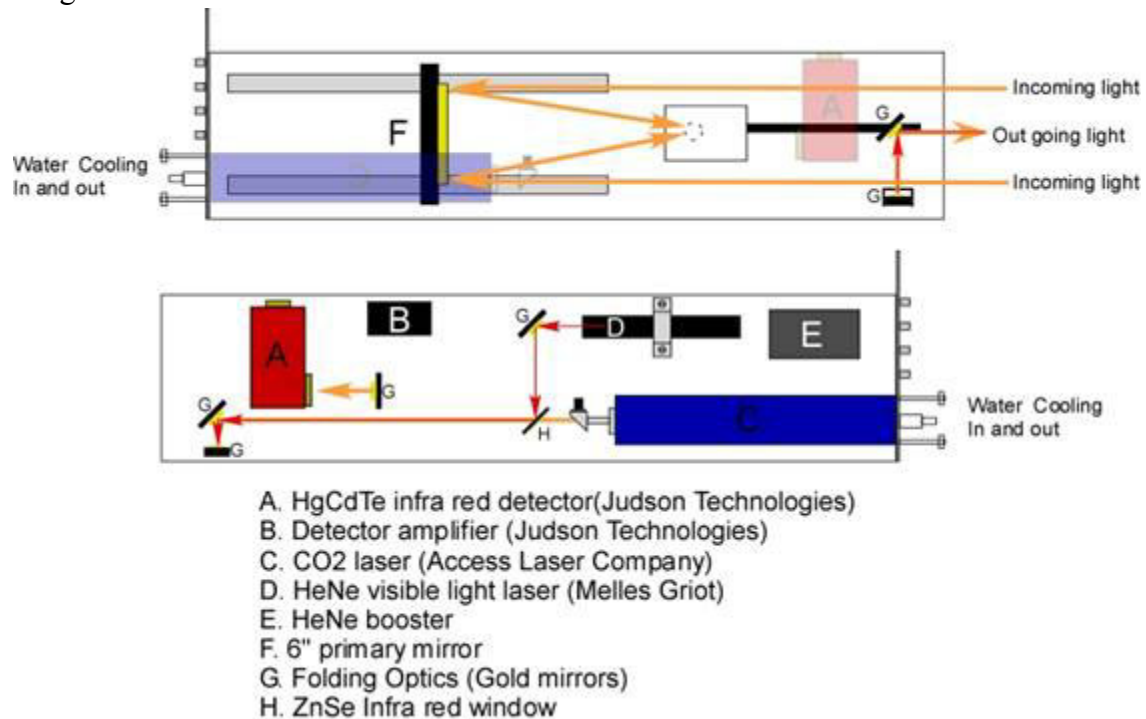


Figure 1 Schematic of Lidar Platform used for Testing and Demonstration of PFT Detection in Air

3.2 Laboratory Testing

For laboratory testing the lidar platform was mounted to a laser table. A one meter test cell was fabricated to contain the PFT tracer during initial bench top testing. The cell consisted of a glass tube fitted with ZnSe windows and valves and both ends of the tube. A photograph of the apparatus is shown in Figure 6. This allowed precise control of the PFT concentration in the air that the lidar was directed through. Air flow was introduced in one valve and exited the second. The air was tagged with PMCH using a BNL PMCH source with a 2 uL/min (vapor) output. The source was placed in a dilution cell to achieve the desired concentration. The dilution cell could be valved out of the air flow loop allowing rapid flushing of the cell. In addition, the air flows to the dilution cell and the

percent of clean air going to the measurement cell could be varied to change the PFT concentration.

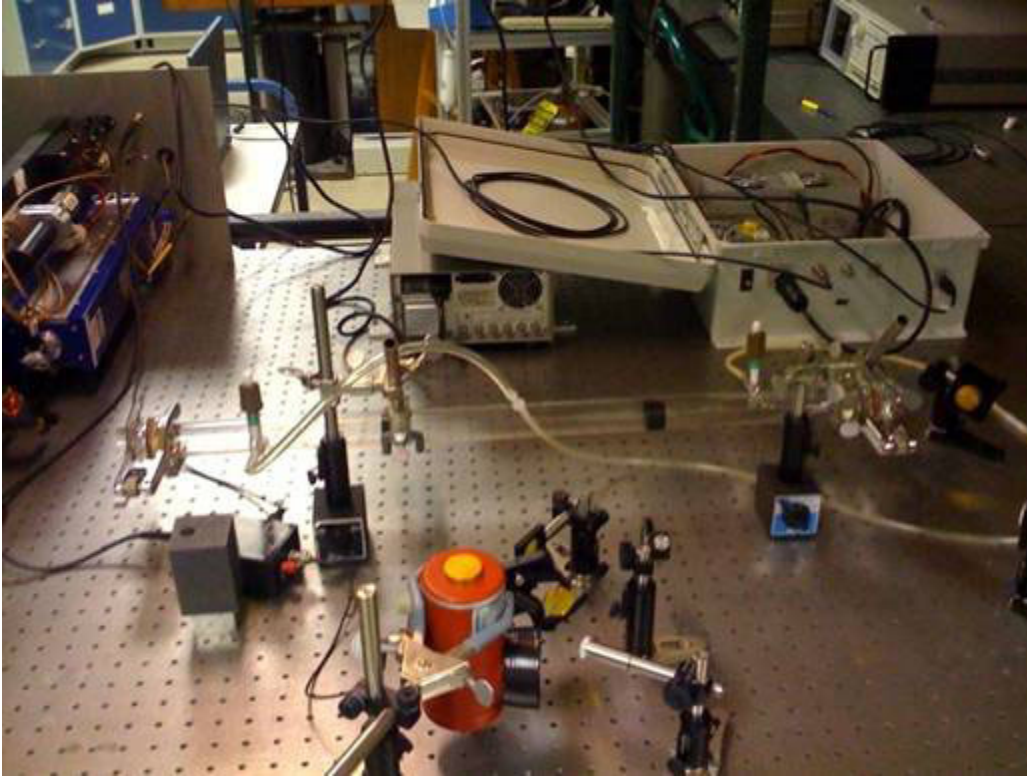


Figure 6 Laboratory Apparatus used in Calibrating PFT Lidar

The laser beam was directed through the cell to a mirror and reflected back to the detector. The initial cell concentration was set at 100 ppb and could not be differentiated from clean air. The concentration was gradually increased until a clear signal decrease was observed. The approximate cell concentration at this point was 20 ppm

Several changes were made to normalize the signal with respect to the laser output. Most importantly was the addition of the laser power meter. However, due to mode fluctuations in the laser and the method in which the signal to the power meter is attenuated we encountered a lower than expected signal to noise ratio (SNR) from the power meter. We removed the attenuator completely and lowered the output from the laser for the bench top experiments and that increased the SNR to a more acceptable level.

It was noted that the power output of the laser varied by widely and appeared to be affected by air conditioning (on versus off) in the laboratory. A fan was added to help cool the laser and that significantly stabilized the laser power. This led to very repeatable results in the calibration tests but, the MDL (1 ppm-m) was not as low as originally achieved on the laser table in previous studies (1 ppb-m). This is believed to be a function of having only a small portion of the laser beam hit the detector. To avoid

saturating the detector, an iris was used in the beam path so only a small segment hit of the beam the detector. An attempt to alleviate this was made by adding a focusing lens and beam splitter. The idea was to focus the return beam and then split some off to avoid saturating the detector. This would allow the whole beam area, albeit weakened by splitting, to hit the detector and avoids fluctuations seen on the fringe of the beam. This achieved an MDL of ~200 ppb-m. While still considerably worse than the original bench top lidar it was a decent improvement. At this point, a decision was made to move the lidar to the indoor test area where the beam could travel 30 to 40 meters, which would reduce the problems with saturation (too much signal return)

3.3 Indoor Testing

The lidar was set up in a high bay area using a brushed aluminum reflector at a distance of 35 meters. With the added beam expander the lidar was directed through an eight inch diameter tube 3 meters long. A PFT source with a release rate of 25 uL/min (vapor) was placed in the center of the tube and the signal to the lidar was monitored to determine at what concentration a discernable signal change occurred. The lidar MDL remained in the 200-300 ppb-m. The results were erratic and appeared to correlate to laser power instability. The temperature in the high bay facility, where testing was conducted, varied much more than the laboratory environment and was higher by 10 to 15 degrees. Even with the added cooling fan the laser output power was deviating excessively.

At this time we received the INEL 13 sources (PMCH) and switched to these sources. Instead of using the tube to contain the PFT in the beam line, the INEL-13 source was placed in a one cubic foot sealed box with the door to the box place parallel to and just below the beam line. This would simulate the opening of a car door. Opening the box 30 minutes after placing the source resulted in a detectable signal. Shorter times produced erratic results which again were correlated to laser power instability. After several tests of on line (absorbing wavelength) and off line (non-absorbing wavelength) measurements, a decision was made to replace the as-received air-cooled plates on the laser with water-cooled plates. The initial test of the laser with water cooling resulted in an order of magnitude better power stability. The laser was then refitted to the lidar platform and testing using the INEL-13 source was repeated. The water cooling greatly improved the detection sensitivity and the PFT was detectable after only a few minutes of the source being placed in the box. However, due to time constraints (demonstration date quickly approaching), testing was moved to the outdoor facility.

3.4 Outdoor Optimization

After final review and approval of the Experimental Safety Review of the outdoor facility, the lidar was moved out to the test facility. Due to safety concerns (the laser was not certified eye safe) the lidar had to be directed to an area with a background that blocked the laser from leaving the test site should a misalignment occur. This resulted in a test path of approximately 100 meters (see Figure 7).

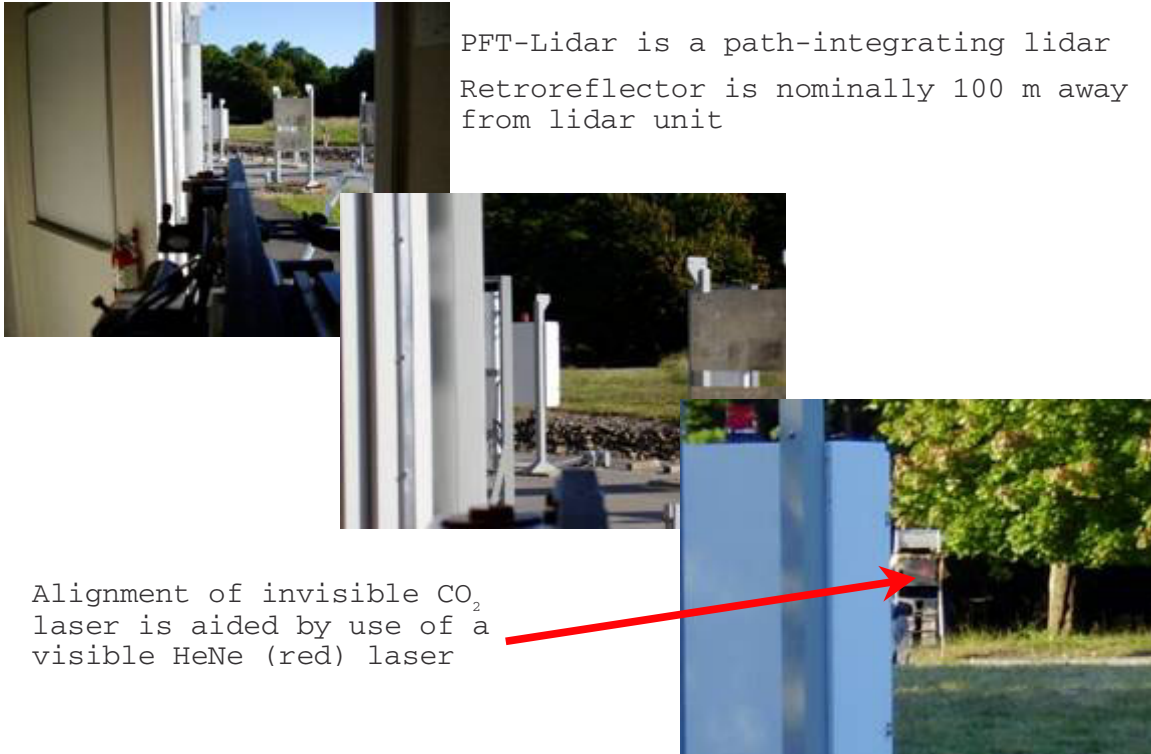


Figure 7 Lidar Test Facility showing Beam Path

The initial test configuration is depicted in Figure 8. A pickup truck was positioned parallel to the beam path. The beam path passed along the driver side of the cab top. To preserve the INEL-18 sources, the first tests were performed by placing 2 to 2.5 mL of PMCH liquid on a napkin and throwing it into the truck and shutting the door. This allowed the PFT concentration to reach a maximum in about 10 to 15 minutes. The lidar was then optimized through several tests using this method.

Initial testing proved the lidar platform to be sensitive to environmental conditions, particularly wind. The lidar platform, electronics and optics were not enclosed (as a commercial unit would be), so a decision was made to place the lidar platform in a trailer and shoot out the door to the target. This reduced the variability considerably. The laser remained very stable and constant with the water cooling and wind protection. The first choice of reflector was an aluminum plate. This resulted in a large signal return that resulted in saturation of the A/D card. This was mainly due to the short path distance being used.

Several tests showed the return power from the laser was consistently too high and the system was “de-tuned” to reduce the signal and keep the A/D card within its limits. Several methods of detuning were tried, including adjusting the collecting mirror, adjusting the reflector surface (angle and type) and modulating the laser power. Eventually the beam telescope was removed and the reflector was changed to a cement block. Using a concrete block had the added benefit of being a more realistic surface for

the target reflector as it would simulate a building face or concrete structure. This resulted in the best stability and reproducibility.

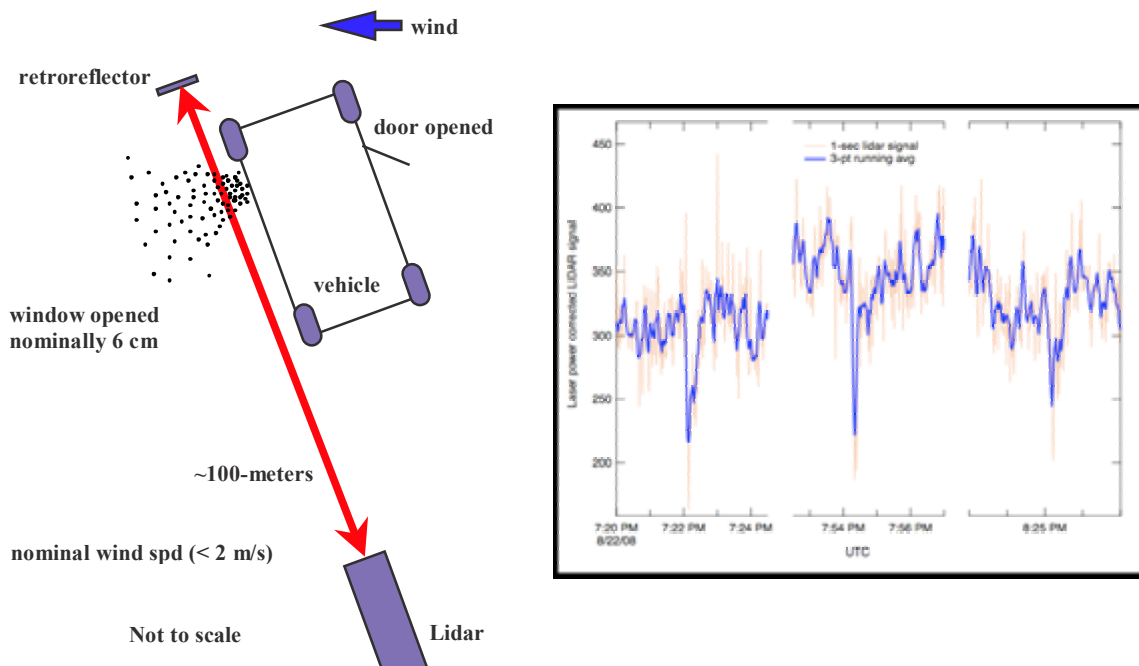


Figure 8 CONOPS for Standoff Detection of PFTs

Testing was then continued using the INEL supplied sources (INEL-18 PMCH @ ~ 550 uL/min vapor). With the system fully tuned the INEL-18 sources produced very large signals from parked cars upon opening the doors. The graph in Figure 8 depicts three iterations of tagging the vehicle. The lidar signal was processed using a notebook computer and labview programming with a graphical interface. An example of the LabVIEW-based GUI is shown in Figure 9 along with the raw traces collected from two vehicle releases following tagging.

Testing on different days and at different times of the day resulted in different signal measurements. Figure 10 shows how wind affects the lidar signal from a vehicle. In these tests the conditions (tagging and delay to door opening) were all the same. Note graph E has a very broad peak that implies the PFT lingers in the area before being blown away by winds, which were calm (<0.4 m/s). Graph B shows results from a night (during the night inversion) when the winds were light (~3 m/s) and changing direction frequently. The detection peak is split into two peaks and broad. The peak diminished and returned to baseline when the car door was closed. Plots A and D are also from light wind days but during the day with fairly constant wind direction and no night inversion. The peaks are narrower and return to baseline more quickly. Plot C was a night time test but the winds were moderate (5.7 m/s). In this case, the peaks from two car releases are narrow and show a rapid decay in the signal after the release (PFTs are swept away quickly).

The remainder of testing was performed to the specifications of the test demo as defined by Tracer Detection Technology Corp., which included placing three cars in the beam path (actually, the beam passed just above the vehicles). Two cars were placed perpendicular to the beam path and the third was placed parallel to the beam. Placing an INEL-18 source in two of the three vehicles, waiting 15 minutes and then opening the doors of the tagged cars one after the other resulted in the data collection depicted in Figure 10, plot C. In this case, the peaks are very well defined and this represents the lidar in its final, fully optimized (to the equipment available) configuration. The lidar is believed to be capable of greater than 0.5 kilometer standoff distances. This is based on the extreme amount of signal return attained (so much that the system had to be de-tuned). This testing was followed by the successful demonstration of the lidar on August 27 at BNL. The results of the demonstration are detailed in the following section.

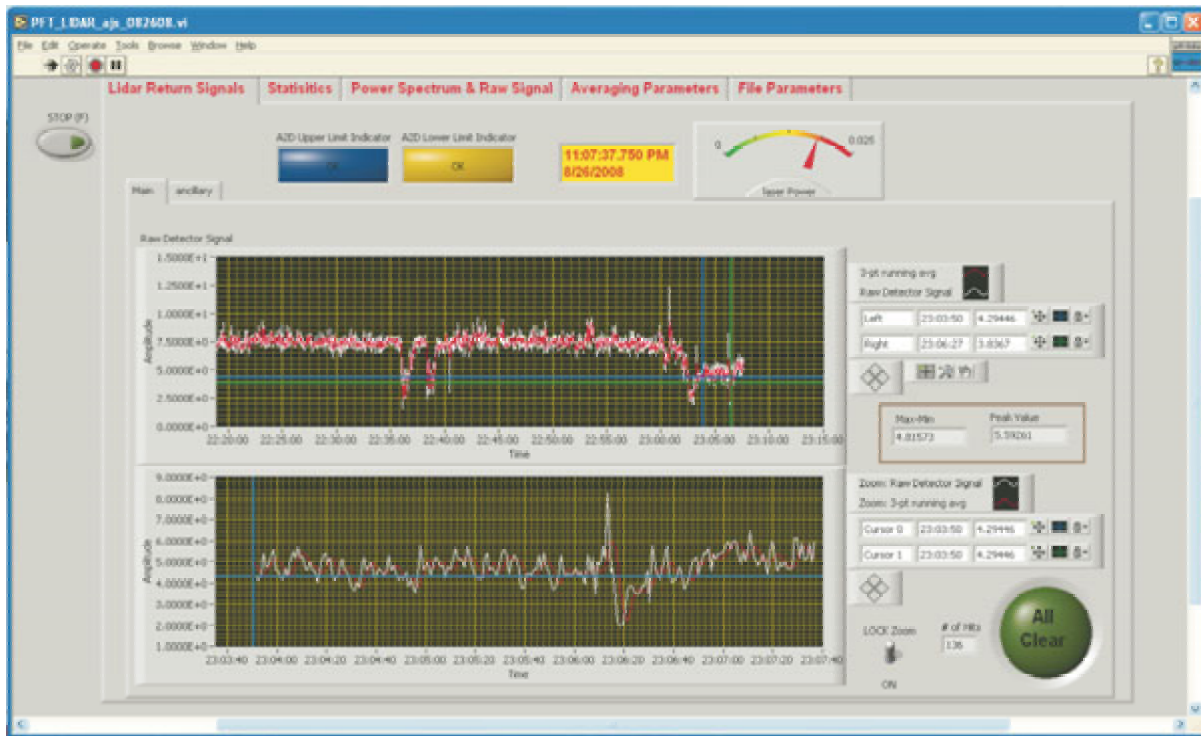


Figure 9 Graphical Interface for PFT Lidar

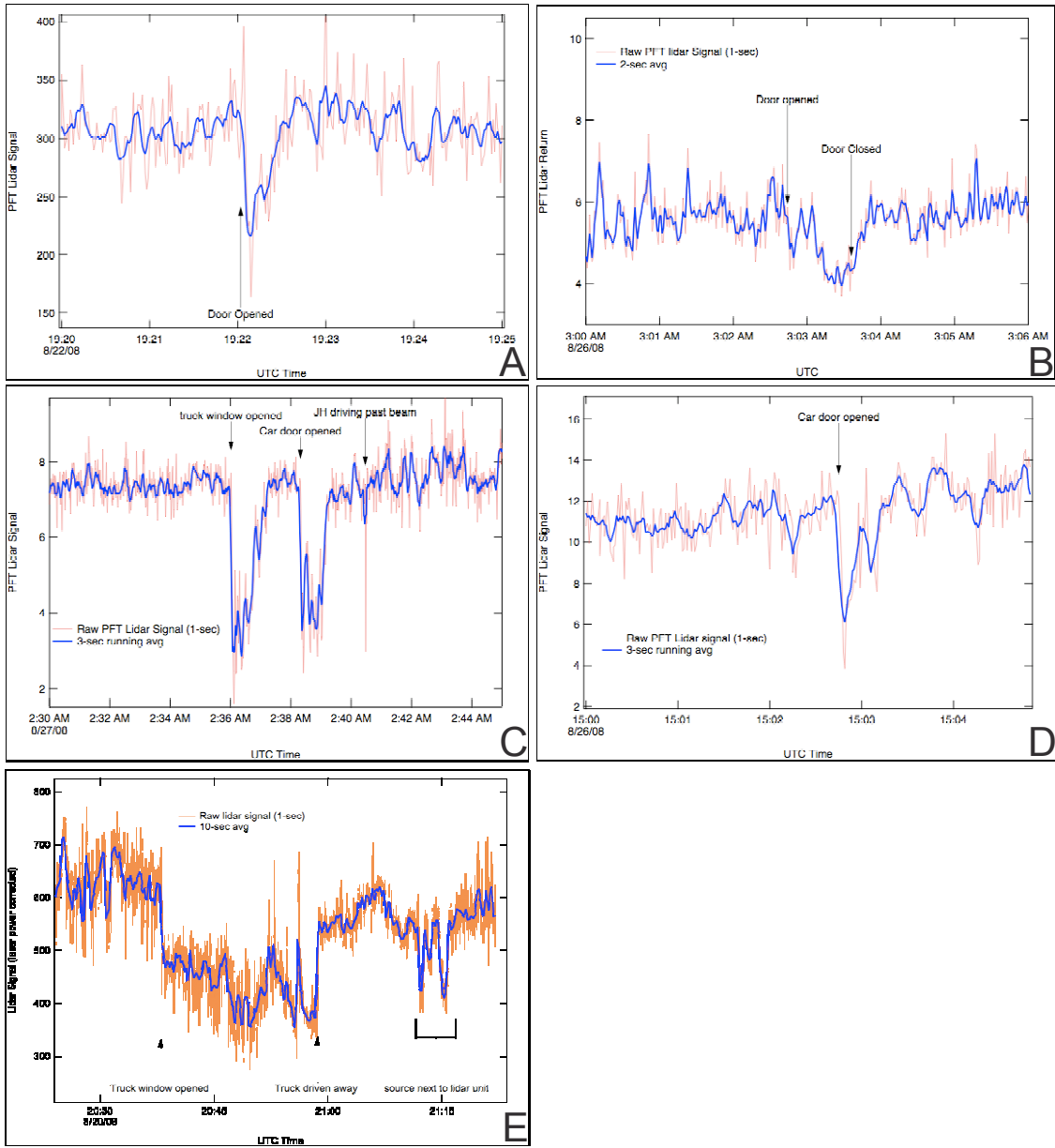
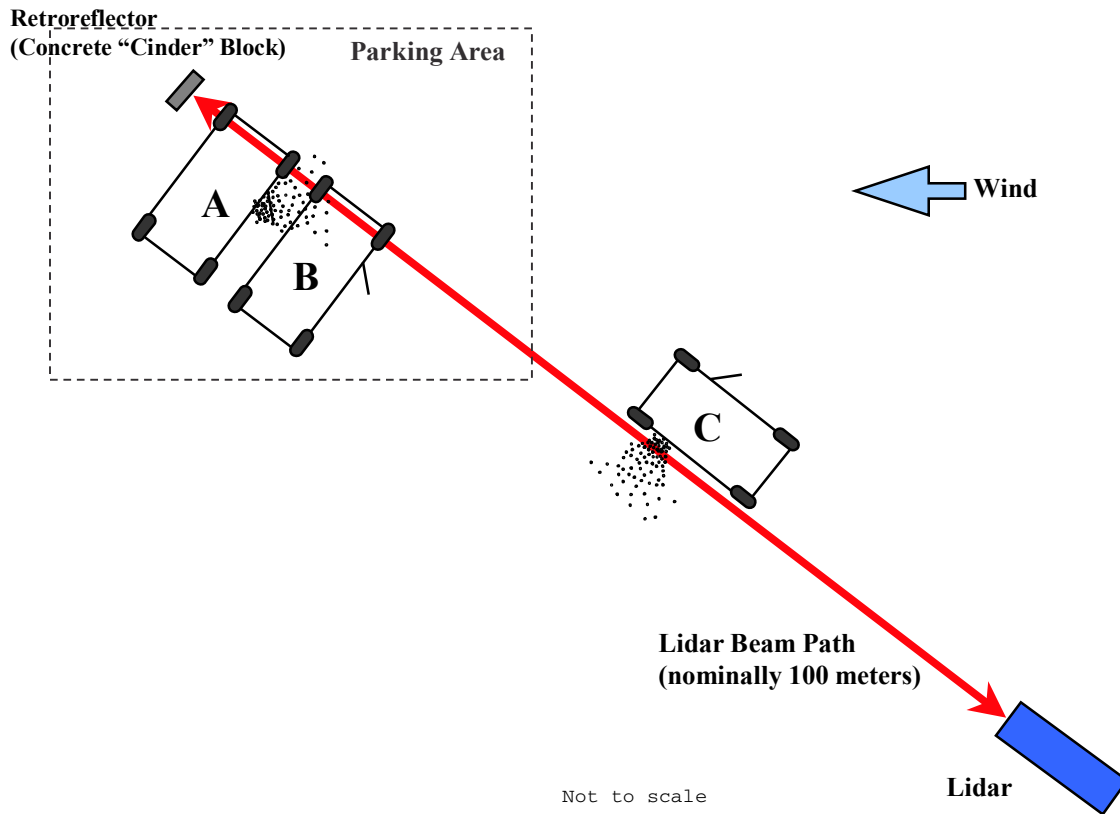


Figure 10 Results of Outdoor Testing of Lidar

4.0 Demonstration Results and Discussion

On August 27, 2008, a demonstration of the lidar detection of PFTs from a vehicle(s) was performed. The test scenario/demonstration was scripted by TDT and included three cars in a parking area/roadway. Two of the cars were parked perpendicular to the beam and once was positioned parallel to the lidar beam path. The configuration is depicted in figure 11.



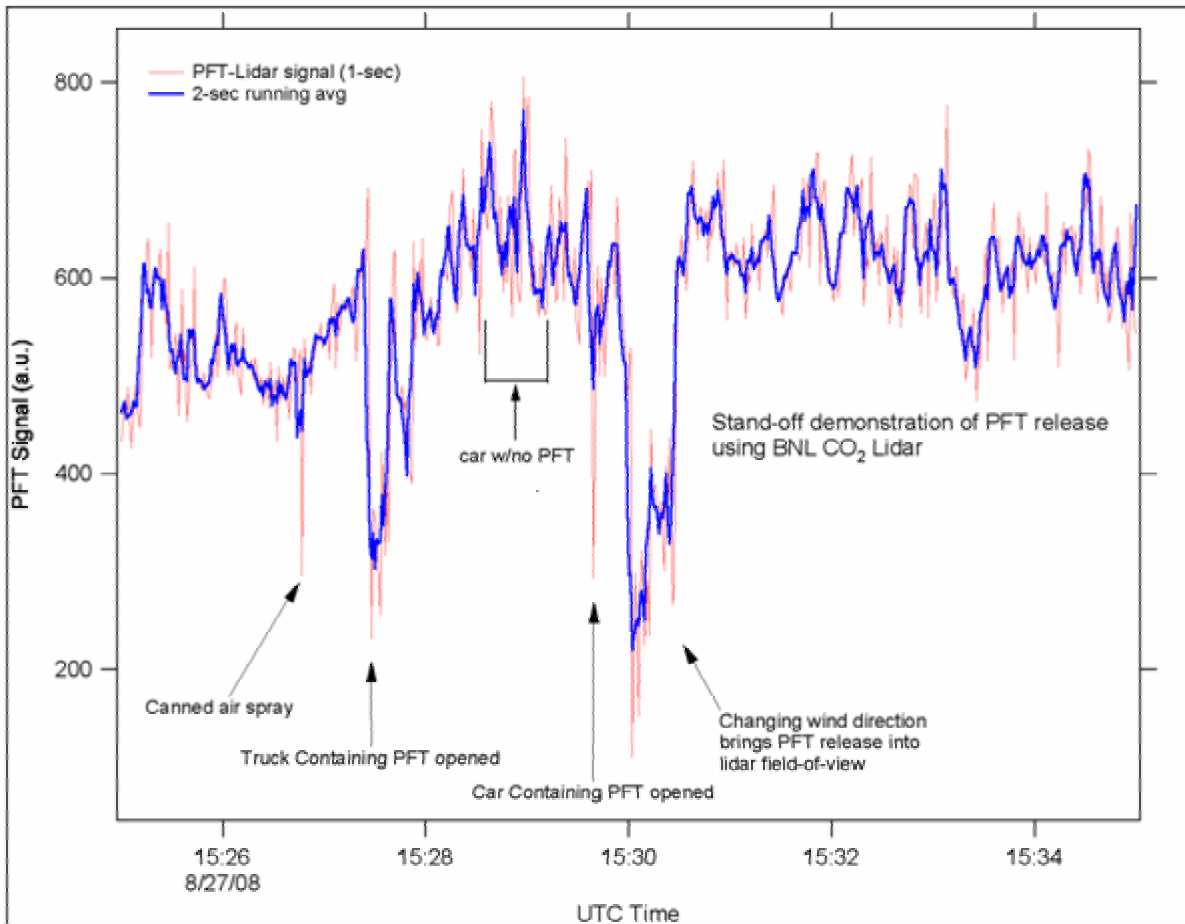
4.1 Results

The demonstration took place approximately 1100 hrs August 27, 2008. Following the TDT demonstration script, at 1055 two of the three vehicles were tagged with PFT sources. Vehicle C was tagged with a napkin with approximately 2 mL liquid PMCH dripped onto it. The napkin was tossed into the vehicle and the door closed. Vehicle A was tagged with an INEL-18 source (PMCH, reservoir ~3 mL, release rate 550 uL vapor/min). The source was opened inside the vehicle and the door closed. Vehicle B was untagged. The lidar operator was unaware of which vehicles were tagged.

At approximately 1127, with the lidar operating, a test using “canned air” (commercial brand used for cleaning computer keyboards, etc.) was done to show the visitors the immediate response of the lidar. One of the lidar team members sprayed a 2 second blast of this “air”, which contains a perfluorocarbon, into the beam path near the reflector

(concrete block). This appears in Figure 12 as a narrow downward peak at ~15:27 (UTC). The red line is the one second lidar signal, while the blue line represents the two-second running average. The blast of canned air was readily apparent, but again was done simply as a demonstration of a definitive response and to show the real-time nature of the detection.

Approximately 30 seconds later a team member opened the door to vehicle C and cracked the driver's side window open nominally 6 cm. An immediate response (Figure 12) was seen as soon as the door was opened and lasted until the door was closed. Thirty seconds after the first vehicle was tested, the door to vehicle B was opened, no response was seen and after 30 seconds the door was closed. Finally, the door to vehicle A was opened just before 1130. An immediate but small peak was seen followed by a very large peak. The member who opened the door noted the wind shifted significantly (swirling gust) just after the door was opened and it is believed this gust carried a larger portion of the PFT plume into the beam path (which was slightly downwind to the beam).



The demonstration was deemed a complete success, in both cases of the tagged vehicles the PFT presence was detected immediately and for the case of the vehicle that was a few

feet downwind of the beam path, the PFT was still seen initially and then very strongly when the wind gusted. For the untagged vehicle no signal was seen.

5.0 Conclusions

The lidar system with the Access MERIT-G laser and water cooling was able to detect PFTs released into a vehicle from a distance of 100 meters. In its final, fully optimized (to the equipment/funding available) configuration the lidar was capable of repeatedly detecting PFTs in the air released from tagged vehicles. Responses were immediate and clear. The demonstration distance was limited by site constraints and in fact, the lidar had to be “de-tuned” and the telescope (beam expander/collimator) was removed to reduce the return signal over such a short distance. Based on this, the lidar is probably capable of greater than 0.5 kilometer standoff distances.

The Access laser is not deemed the best suited for this application as the power stability is lacking. It is believed the MDL (~200 ppb-m) suffered because of this instability. The lidar also suffered from not being enclosed in a housing (time and funding constraints).

In addition, the lidar was fixed in place rather than used in a scanning mode. This was due to the inability to easily normalize out background reflectivity differences that would be seen when scanning across an area.

6.0 Recommendations

The current MDL needs to be improved by at least two orders of magnitude to make the system capable of detecting a PFT source of a more realistic size (one that would last days or weeks). Based on the original laboratory experiments (table top lidar from prior work), the MDL may be capable of being lowered to 1 ppb-m. In addition, to be practical under a real world conditions, the lidar needs to be capable of operating in a scanning mode.

The current configuration of lidar will not likely attain this detection limit nor can it operate in a scanning configuration. To improve the system several changes need to be made. The most obvious is the purchase of a better quality laser. This will provide much greater system stability, would have system feedback, and could allow auto wavelength tuning and/or thermoelectric cooling (to reduce package size).

The biggest engineering change would be the addition of a second laser. By adding a second laser the lidar can look on and off wavelength simultaneously (at the same target and over the same time period). This will improve the sensitivity and allows common mode noise reduction and would allow the use of the lidar in a scanning configuration. A schematic of a two laser lidar is depicted in Figure 13. A two laser system could also (by purchasing a scanning wavelength laser for the on wavelength laser) be configured to reduce false positives to near zero. If detection occurs, the laser could be rapidly (milliseconds) retuned to a secondary absorbing wavelength. Non-PFT interferences, which would not absorb at this second wavelength, could be ignored. This might also

allow the use of multiple PFT taggants and each would have a characteristics fingerprint in the IR absorption spectra. If enough points on the spectra can be determined by wavelength scanning then individual PFTs might be simultaneously detected.

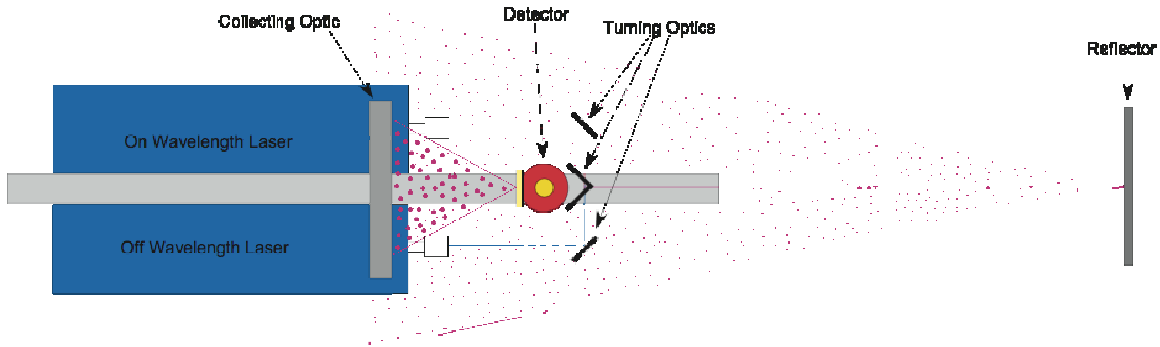


Figure 13 Dual Wavelength (dual laser) Lidar for PFT Stand-off Detection

Finally, if funding allowed, a heterodyning CO2 lidar and/or off-axis optical configuration might be designed. Heterodyning would provide range resolved PFT detection while an off-axis optical configuration (shown in Figure 14) would remove shadowing of the return signal and greatly improve the near field detection sensitivity.

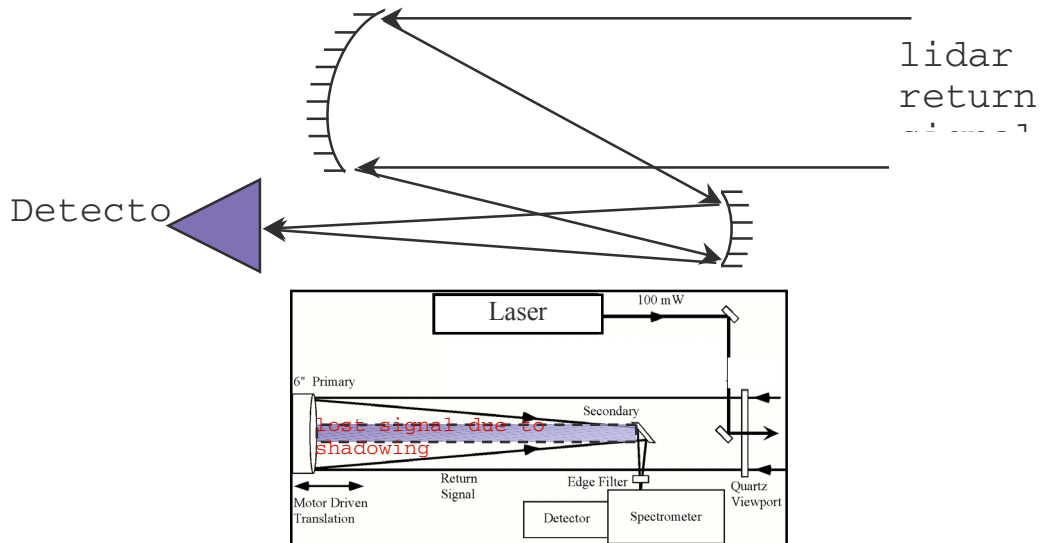


Figure 14 Off Axis Optical Lidar Configuration versus Standard Lidar Configuration

7.0 References

- ¹ Heiser, J.H. and Sedlacek, A.J., “Using Lidar to Measure Perfluorocarbon Tracers for the Verification and Monitoring of Cap and Cover Systems”, *Water, Air, & Soil Pollution*, 2005.
- ² Wu, M., Ray, M., Fung, K. H., Ruckman, M. W., Harder, D. and Sedlacek, A. J., Stand-off Detection of Chemicals UV Raman Spectroscopy, *Appl. Spec.* 54, 800 (2000).
- ³ Ray, M., Sedlacek, A. J. and Wu, M., Ultraviolet mini-Raman lidar for stand-off, in situ identification of chemical surface contaminants, *Rev. Sci. Instru.* 71, 3485 (2000).
- ⁴ Milton, M. J. T., Woods, P. T., Jolliffe, B. W., Swann, N. R. W. and McIlveen, T. J.; 1992, *Appl. Phys. B* **55**, 41.
- ⁵ Rothe, K. W., Brinkmann, U. and Walther, H.; 1974, *Appl. Opt.* 4, 181.
- ⁶ Oh, C., Prasad, C. R., Fromzel, V., Hwang, I. H., Reagan, J. A., Fang, H. and Rubio, M.; 1999, *Proceedings of the SPIE Conference on Laser Radar Technology 3707*, 17186.
- ⁷ Edner, H.; 1995, *Review of Laser Engineering* 23, 142.
- ⁸ Edner, H., Faris, G. W., Sunesson, A. and Svanberg, S.; 1989, *Appl. Opt.* 28, 921.
- ⁹ Chyba, T. H., Zenker, J. T., McCray, C. L., Lee, H. R., Elivert, R., Thomas, B., Toppin, C., Larson, D., Higdon, N. S. and Ritcher, D. A.; 1999, *SPIE Proceedings 3757*, 80.
- ¹⁰ Sunesson, J. A., Apituley, A.; and Swart, D. P. J. 1993, *Appl. Opt.* 33, 7045.
- ¹¹ Papayannis, A., Ancellet, G., Pelon, J. and Megie, G.; 1989, *Appl. Opt.* 29, 467.